Supporting Information

Zhang et al. 10.1073/pnas.1121606109

SI Results

The lead agent, S3I-201.1066 (1), is a moderately potent signal transducer and activator of transcription (Stat)3 Src homology (SH)2 domain-binding ligand (2) and accesses the three solvent-accessible subpockets on the SH2 domain surface. We hypothesized that improved binding to the third pocket would enhance inhibitory activity. By extensive structure–activity relationship analysis of S3I-201.1066 and analogs structurally designed with appendages that promote interactions with all of the three subpockets on the Stat3 SH2 domain surface, BP-1-102 (Fig. 1*A*) was identified. BP-1-102 has appendages that promote interactions with all three subpockets (Fig. 1*B*). It retains the 4-aminosalicylic acid group as an effective phosphotyrosine (pTyr) mimetic (2), which binds to the pTyr-binding portion of the SH2 domain, making interactions with Lys591, Glu594, and Arg609 (Fig. 1*B*), and contains the hydrophobic cyclohexylbenzyl substituent, which forms van der Waals interactions with a series of predominantly hydrophobic residues, including Val637, Ile659, and Trp623 (Fig. 1*B*) that comprise the pY+1 (Leu)-binding pocket. The key modification is the pentafluorobenzene sulfonamide component of the molecule, linked via a glycine unit to the salicylic acid, which interacts with the previously unexplored third subpocket composed of Lys591, Glu594, Ile634, and Arg595 (Fig. 1*B*). Critically, the pentafluorobenzene may better interact with the Stat3 SH2 domain surface by participating in hydrogen bonds and also better interacting with the charged Lys side chain, as previously noted in a different context (3). The more polar pentafluorobenzene unit also confers enhanced solubility and oral bioavailability.

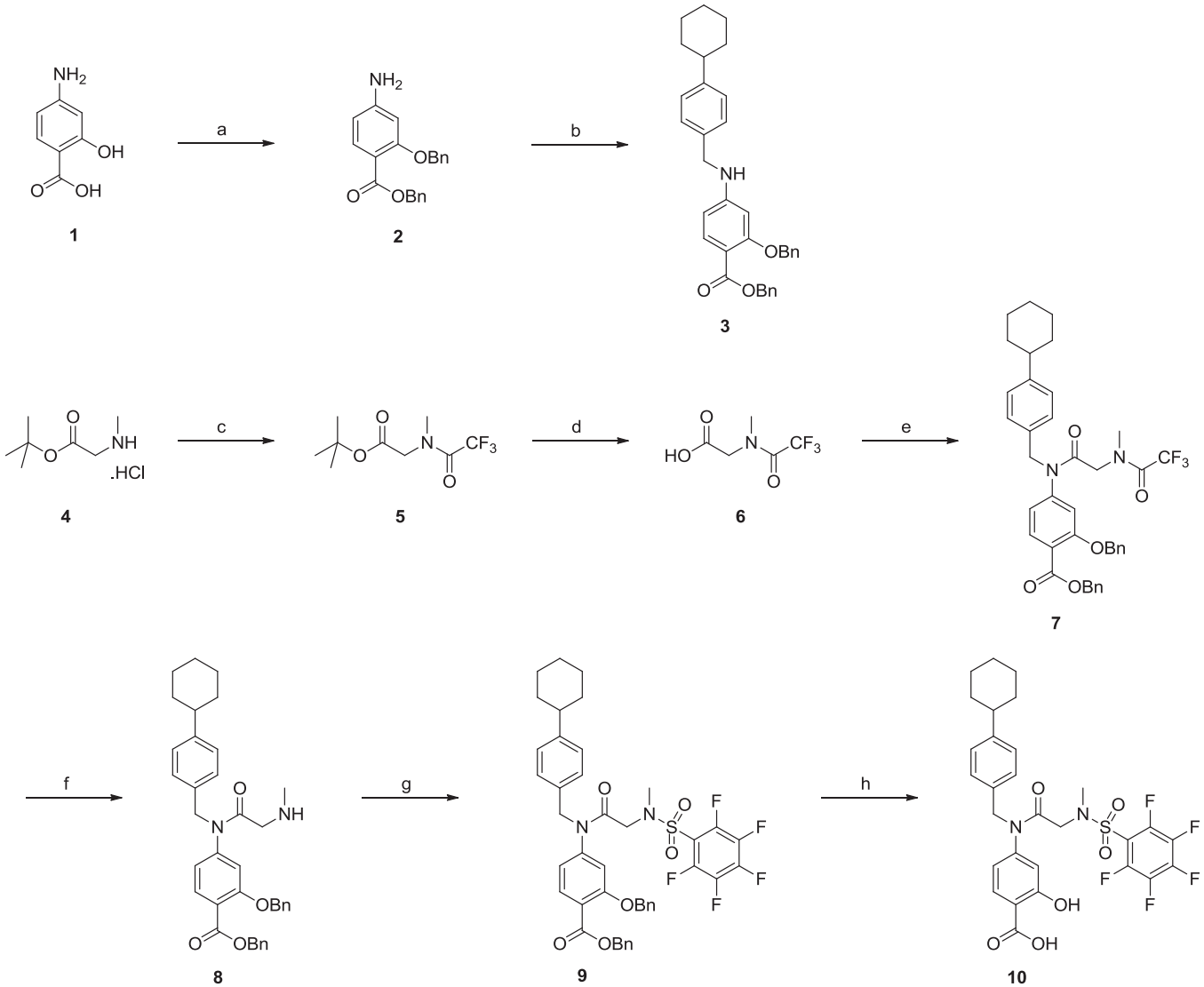

Scheme S1. (*A*) BnBr (2 equivalents), KO^{t}Bu, DMF, 0 °C, 16 h, 73%. (*B*) 4-Cyclohexylbenzaldehyde, AcOH, $NaCNBH_3$, room temperature (rt), 16 h, 79%. (*C*) $(CF_3CO)_2O$, DIPEA (diisopropylethylamine), CH_2Cl_2, rt, 3 h, 96%. (*D*) TFA/CH_2Cl_2, 1:1, rt, 5 h, 100%. (*E*) **3**, PPh_3Cl_2, $CHCl_3$, 60 °C, 12 h, 97%. (*F*) LiOH·H_2O, THF/H_2O, 3:1, rt, 10 min, 98%. (*G*) PhF_5SO_2Cl, DIPEA, CH_2Cl_2, rt, 16 h, 93%. (*H*) H_2, 10% Pd/C, MeOH/THF, 1:1, rt, 16 h, 95%.

SI Materials and Methods

Chemical Methods. Anhydrous solvents—methanol, DMSO, CH_2Cl_2, THF, and dimethylformamide (DMF)—were purchased from Sigma-Aldrich and used directly from Sure/Seal bottles. Molecular sieves were activated by heating to 300 °C under vacuum. All reactions were performed under an atmosphere of dry nitrogen in oven-dried glassware and were monitored for completeness by TLC (visualized by UV light, or developed by treatment with $KMnO_4$ stain or phosphomolybdic acid stain). ^1H and ^{13}C NMR spectra were recorded on a Bruker 400 MHz spectrometer in either $CDCl_3$, CD_3OD, or d_6-DMSO. Chemical shifts (δ) are reported in parts per million after calibration to residual isotopic solvent. Coupling constants (J) are reported in Hz. Before biological testing, inhibitor purity was evaluated by reversed-phase HPLC (rpHPLC). Analysis by rpHPLC was performed using a Microsorb-MV 300 A C18 250 mm × 4.6 mm column (Agilent) run at 1 mL/min and using gradient mixtures. The linear gradient consisted of a changing solvent composition of (*i*) 100% H_2O (0.01 M NH_4OAc) for 2 min to 100% MeOH at 25 min and UV detection at 254 nm and (*ii*) 100% H_2O (0.01 M NH_4OAc) for 2 min to 100% MeOH at 62 min and UV detection at 254 nm, each ending with 5 min of 100% MeOH. For reporting rpHPLC data, percentage purity is given in parentheses after the retention time for each condition.

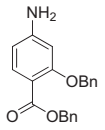

(2) Benzyl 4-amino-2-(benzyloxy)benzoate. To a stirred solution of 4-aminosalicylic acid (**1**) (3.00 g, 19.6 mmol) in DMF (0.1 M) at 0 °C was added KO^{t}Bu (2.42 g, 21.6 mmol). After 15 min, benzyl bromide (2.57 mL, 21.6 mmol) was added dropwise. The suspension was allowed to stir at room temperature (rt) for a further 4 h before the reaction vessel was again cooled to 0 °C. A further 1.1 equivalents of KO^{t}Bu (2.42 g, 21.6 mmol) were added before the dropwise addition of benzyl bromide (2.57 mL, 21.6 mmol). The reaction was then stirred overnight before quenching with H_2O. The solution was then repeatedly extracted with ethyl acetate and the organics were combined. The organics were then washed with H_2O and brine and dried over Na_2SO_4 and concentrated in vacuo (3.40 g, 74%): δ_H (400 MHz, d_6-DMSO) 5.07 (s, 2H, CH_2), 5.21 (s, 2H, CH_2), 5.99 (br s, 2H, NH_2), 6.18 (dd, J = 8.6 and 1.8 Hz, 1H, CH), 6.32 (d, J = 1.7 Hz, 1H, CH), 7.28–7.38 (8H, m, CH), 7.47 (d, J = 7.2 Hz, 2H, CH), 7.60 (d, J = 8.6 Hz, 1H, CH); δ_C (100 MHz, d-$CDCl_3$) 65.8, 70.2, 99.1, 106.7, 109.0, 126.3, 126.8, 127.5, 127.7, 127.9, 128.1, 128.3, 128.4, 134.3, 136.6, 136.7, 152.2, 160.7, 165.7; LRMS (low-resolution mass spectrometry) (ES+) calculated for [$C_{21}H_{19}NO_3$ + H] 334.14, found 334.17.

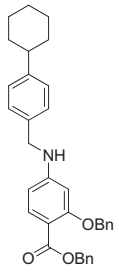

(3) Benzyl 2-(benzyloxy)-4-(4-cyclohexylbenzylamino)benzoate. To a solution of primary aniline (**2**) (1.7 g, 5.0 mmol) and acetic acid (0.36 g, 6.0 mmol) stirred in anhydrous MeOH (0.1 M) with 4-Å molecular sieves was added 4-cyclohexylbenzaldehyde (1.0 g, 5.5 mmol). The solution was then heated to 45 °C for 3 h and allowed to cool to rt. Next, $NaCNBH_3$ (0.47 g, 7.5 mmol) was added and the reaction was allowed to stir at rt overnight. When TLC indicated the reaction was complete, the reaction was diluted with CH_2Cl_2, filtered, and concentrated in vacuo. The crude product was dissolved in CH_2Cl_2, washed with saturated $NaHCO_3$, H_2O, and brine, and then dried over Na_2SO_4. Compound **3** was isolated using flash chromatography in a mixture of CH_2Cl_2 and EtOAc (2.4 g, 83%): δ_H (400 MHz, d-$CDCl_3$) 1.25–1.48 (m, 5H, CH_2), 1.74–1.95 (m, 5H, CH_2), 2.48–2.52 (m, 1H, CH), 4.28 (s, 2H, CH_2), 4.49 (br s, 1H, NH), 5.08 (s, 2H, CH_2), 5.32 (s, 2H, CH_2), 6.17 (d, J = 2.0 Hz, 1H, CH), 6.21 (dd, J = 8.6 and 2.0 Hz, 1H, CH), 7.19–7.27 (m, 4H, 4 CH), 7.28–7.37 (m, 6H, 6 CH), 7.40–7.49 (m, 4H, 4 CH), 7.85 (d, J = 8.6 Hz, 1H, 1 CH); δ_C (100 MHz, d-$CDCl_3$) 26.0, 26.7, 34.3, 44.1, 47.3, 65.7, 70.3, 97.1, 104.8, 108.2, 126.8, 127.0, 127.4, 127.5, 127.6, 127.9, 128.2, 128.3, 134.2, 135.4, 136.7, 136.8, 147.4, 152.9, 160.8, 165.8; LRMS (ES+) calculated for [$C_{34}H_{35}NO_3$ + H] 506.27, found 506.22.

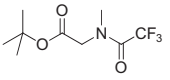

(5) tert-Butyl 2-(2,2,2-trifluoro-N-methylacetamido)acetate. To a stirred solution of *tert*-butyl 2-(methylamino)acetate (2.00 g, 11 mmol) and DIPEA [3.65 g (4.80 mL), 27.5 mmol] in $CHCl_3$ (0.1 M) was added triflic anhydride (2.54 g, 12.1 mmol). The solution was allowed to stir at rt for 3 h before quenching with water and extraction into CH_2Cl_2. The combined organic layers were washed with water and brine and dried over Na_2SO_4, and the solution was concentrated under reduced pressure to give **5** (1.44 g, 88%): δ_H (400 MHz, d-$CDCl_3$) 1.46 (s, 9H, 3 CH_3), 3.08 (s, 1H, CH_3), 3.18 (s, 2H, CH_3), 4.04 (s, 2H, CH_2).

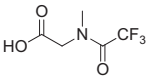

(6) 2-(2,2,2-Trifluoro-N-methylacetamido)acetic acid. *tert*-Butyl ester **5** (2.00 g, 11.0 mmol) was dissolved in a TFA:CH_2Cl_2 (1:1) solution (0.1 M) and allowed to stir for 5 h at rt. The product was then concentrated under reduced pressure to yield pure compound **6** (2.50 g, 95%): δ_H (400 MHz, d-$CDCl_3$) 3.22 (s, 3H, CH_3), 4.19 (s, 2H, CH_2).

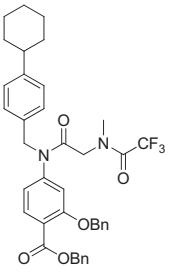

(7) Benzyl 2-(benzyloxy)-4-(N-(4-cyclohexylbenzyl)-2-(2,2,2-trifluoro-N-methylacetamido)acetamido)benzoate. To a stirred solution of the secondary aniline **3** (0.70 g, 1.4 mmol) and carboxylic acid **6** (0.28 g, 1.5 mmol) in $CHCl_3$ (0.1 M) was added PPh_3Cl_2 (1.2 g,

3.4 mmol). The reaction was then heated to 60 °C and stirred overnight. The reaction was allowed to cool and the solvents were removed under reduced pressure. The concentrate was absorbed directly onto silica for column chromatography (hexanes:EtOAc 2:1) purification yielding compound **7** (0.91 g, 97%): δ_H (400 MHz, $CDCl_3$) 1.35–1.44 (m, 5H, CH_2), 1.71–1.90 (m, 5H, CH_2), 3.17 (m, 4H, CH_3, CH), 3.79 (s, 2H, CH_2), 4.84 (s, 2H, CH_2), 4.97 (s, 2H, CH_2), 5.35 (s, 2H, CH_2), 6.65 (s, 1H, CH), 6.78 (dd, J = 8.4 and 1.6 Hz, 1H, CH), 7.10–7.19 (m, 4H, CH), 7.29–7.43 (m, 10H, CH), 7.86 (d, J = 8.4 Hz, 1H, CH); δ_C (100 MHz, $CDCl_3$) 25.8, 26.6, 34.2, 36.7, 44.0, 51.2, 52.6, 66.7, 70.4, 77.2, 113.9, 115.0, 117.6, 119.8, 126.8, 126.9, 127.7, 128.0, 128.3, 128.3, 128.4, 128.6, 132.9, 133.6, 135.5, 135.6, 144.6, 147.5, 157.0, 158.4, 165.1, 165.4; LRMS (ES+) calculated for [$C_{39}H_{39}F_3N_2O_5$ + Na] 695.27, found 695.36.

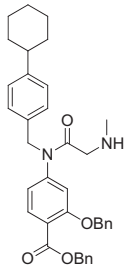

(8) Benzyl 2-(benzyloxy)-4-(N-(4-cyclohexylbenzyl)-2-(methylamino)-acetamido)benzoate. Compound **7** (2.68 mmol) was dissolved in a THF:H_2O (3:1) solution and treated with LiOH·H_2O (337 mg, 8.04 mmol). After 10 min, the reaction was completed and diluted with H_2O. The product was extracted into EtOAc and the combined extracts were washed with saturated $NaHCO_3$, H_2O, and brine and dried over Na_2SO_4 and concentrated under reduced pressure to yield **8** (1.57 g, 99%): δ_H (400 MHz, $CDCl_3$) 1.35 (m, 5H, CH_2), 1.66–1.84 (m, 5H, CH_2), 2.28 (s, 2H, CH_3), 2.44 (m, 1H, CH), 3.02 (s, 2H, CH_2), 4.81 (s, 2H, CH_2), 4.89 (s, 2H, CH_2), 5.30 (s, 2H, CH_2), 6.52 (s, 1H, CH), 6.54 (d, 1H, J = 8.0 Hz, CH), 7.05–7.13 (m, 4H, CH), 7.24–7.37 (m, 12H, CH), 7.80 (d, J = 8.0 Hz, 1H, CH); δ_C (100 MHz, $CDCl_3$) 25.6, 26.3, 34.0, 35.4, 43.7, 52.0, 52.2, 66.4, 70.0, 77.2, 113.6, 119.6, 119.9, 126.4, 126.6, 127.5, 127.6, 127.7, 128.0, 128.1, 128.3, 132.5, 133.9, 135.3, 135.43, 145.0, 147.0, 158.1, 164.8, 169.6; LRMS (ES+) calculated for [$C_{37}H_{40}N_2O_4$ + H] 577.31, found 577.45.

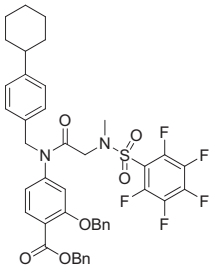

(9) Benzyl 2-(benzyloxy)-4-(N-(4-cyclohexylbenzyl)-2-(2,3,4,5,6-pentafluoro-N-methylphenylsulfonamido)acetamido)benzoate. To a stirred solution of amine (**8**) (55 mg, 0.1 mmol) dissolved in CH_2Cl_2 (0.1 M) was added DIPEA (*N*,*N*-diisopropylethylamine) (16.3 mg, 0.13 mmol) and pentafluorobenzenesulfonyl chloride (28.2 mg, 0.11 mmol). After 1 h, the reaction was diluted with CH_2Cl_2, washed with water followed by a brine wash, and dried over Na_2SO_4. The organic layer was then concentrated under reduced pressure and purified by silica gel column chromatography to yield **9** (49 mg, 63%): δ_H (400 MHz, *d*-$CDCl_3$) 1.34–1.42 (m, 5H, CH_2), 1.70–1.86 (m, 5H, CH_2), 2.43–2.52 (m, 1H, CH), 3.05 (s, 3H, CH_3), 3.86 (s, 2H, CH_2), 4.67 (s, 2H, CH_2), 4.94 (s, 2H, CH_2), 5.35 (s, 2H, CH_2), 6.44 (s, 1H, CH), 6.66 (d, J = 8.0 Hz, 1H, CH), 6.96 (d, J = 7.2 Hz, 2H, CH), 7.12 (d, J = 7.2 Hz, 2H, CH), 7.30–7.41 (m, 10H, CH), 7.84 (dd, J = 8.0 and 1.2 Hz, 1H, CH); δ_C (100 MHz, *d*-$CDCl_3$) 26.0, 26.7, 34.4, 35.4, 44.1, 51.9, 52.7, 67.0, 70.70, 111.8, 114.0, 115.8, 119.9, 121.1, 127.0, 127.1, 128.1, 128.2, 128.2, 128.5, 128.6, 128.7, 133.3, 133.4, 135.6, 135.6, 137.8, 141.6, 142.9, 144.2, 147.9, 158.7, 165.2, 165.8; LRMS (ES+) calculated for [$C_{43}H_{39}F_5N_2O_6S$ + H] 807.84, found 807.79.

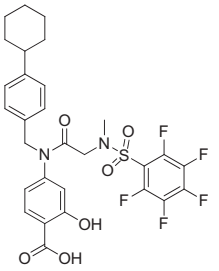

(10) 4-(N-(4-Cyclohexylbenzyl)-2-(2,3,4,5,6-pentafluoro-N-methylphenylsulfonamido)acetamido)-2-hydroxybenzoic acid. Benzyl-protected **10** (48.5 mg, 0.06 mmol) was dissolved in a mixture of THF:MeOH (1:1). The solution was degassed thoroughly before careful addition of catalytic 10% Pd/C (6 mg, 10 mg/mmol). The system was thoroughly flushed with H_2 gas and stirred under an H_2 gas atmosphere for 3 h. Upon completion, the reaction mixture was filtered (to remove Pd/C), concentrated, and purified by silica gel chromatography to give **10** (37 mg, 99%): δ_H (400 MHz, d_6-DMSO) 1.27–7.41 (m, 5H, CH_2), 1.64–1.79 (m, 5H, CH_2), 2.40–2.49 (m, 1H, CH), 3.00 (s, 3H, CH_3), 4.13 (s, 2H, CH_2), 4.77 (s, 2H, CH_2), 6.74 (dd, J = 8.4 and 2.0 Hz, 1H, CH), 6.83 (d, J = 2.0 Hz, 1H, CH), 7.04 (d, J = 8.0 Hz, 2H, CH), 7.12 (d, J = 8.0 Hz, 2H, CH), 7.80 (d, J = 8.4 Hz, 1H, CH); δ_C (100 MHz, d_6-DMSO) 25.4, 26.2, 33.8, 35.5, 43.2, 51.2, 51.7, 116.1, 118.4, 118.8, 126.5, 127.5, 131.4, 133.9, 146.3, 146.5, 161.5, 165.9, 171.0; HRMS (high-resolution mass spectrometry) (ES+) calculated for [$C_{29}H_{27}F_5N_2O_6S$ + H] 627.1582, found 627.1551; HPLC (I) t_R = 22.71 min (97.47%), (II) t_R = 39.92 min (95.22%).

Identification of Putative Stat3 Binding Sites in the Human Krüppel-Like Factor 8 Promoter. The human Krüppel-like factor (KLF)8 promoter sequence (−441 to +946; GenBank accession no. NM_007250.4) was searched, and three putative Stat3 binding sites [TTAGCATAA (−253 to −245), TTCGCTGAA (+217 to +225), and TTCTACCAA (+260 to +268)] were selected for further investigation into Stat3 DNA-binding activity by electrophoretic mobility shift assay (EMSA) analysis. The ^{32}P-labeled oligonucleotide probes used in the assay, with putative Stat3 binding sites underlined, are 5′-AGCTGGAGAA<u>TTAGCATAA</u>CCG-GAGT-3′, 5′-AGCTGCCATTT<u>TTCGCTGAA</u>GCCCCTG-3′, and 5′-AGCTCTATGA<u>TTCTACCAA</u>TCGTCGG-3′. Oligonucleotide sequences were purchased from Invitrogen.

Cloning of pXJ-Flag-Stat3 SH2 Domain and Site-Directed Mutagenesis of the KLF8 Promoter. The DNA fragment of Stat3 SH2 domain (residues 582–668) flanked by BamHI at the 5′ end and KpnI at the 3′ end was cloned into pXJ40-FLAG [a kind gift of X. Cao, Institute of Molecular and Cellular Biology, Singapore (4, 5)]. The new construct was confirmed by sequencing. The human KLF8 promoter-driven luciferase reporter construct pLucKLF8 was previously described (6). The putative Stat3 binding site <u>T</u>TAG-CATAA (−253 to −245) in the human KLF8 promoter (GenBank accession no. NM_007250.4) was mutated to <u>G</u>TAGCATAA us-

ing Stratagene's QuikChange Lightning Site-Directed Mutagenesis Kit (Agilent Technologies) and following the manufacturer's instructions to generate pLucKLF8/−253T/G.

Nuclear Extract Preparation, EMSA, and Densitometric Analysis. Nuclear extract preparations and EMSA analysis were carried out as previously described (1, 7–9). The ^{32}P-labeled oligonucleotide probes used were hSIE (high-affinity *sis*-inducible element from the *c-fos* gene, m67 variant, 5′-AGCTTCATTTCCCGTAAATCCCTA-3′) that binds Stat1 and Stat3 (8, 10) and the mammary gland factor element from the bovine β-casein gene promoter (sense strand, 5′-AGATTTCTAGFAATTCAA-3′) that binds Stat5 (11, 12). For the direct effect of BP-1-102 on STAT DNA-binding activity, nuclear extracts containing activated STATs prepared from NIH 3T3/v-Src or EGF-stimulated NIH 3T3/hEGFR cells were preincubated with the agent for 30 min at room temperature before incubation with the radiolabeled probe for 30 min at 30 °C before subjection to EMSA analysis. Where appropriate, supershift analysis was performed in which nuclear extracts were preincubated with the anti-Stat3 antibody directed against Stat3 N-terminal amino acid residues 5–240 (F-2) (Santa Cruz Biotechnology) before incubation with the radiolabeled probe. Bands corresponding to DNA-binding activities for each concentration of BP-1-102 were scanned and quantified using ImageQuant (GE Healthcare) and plotted as a percentage of control (vehicle) against concentration of BP-1-102; IC_{50} values were derived from these plots, as previously reported (13, 14).

Transient Transfection of Cells, Treatment with BP-1-102, and in Vitro Studies. Transient transfection and luciferase assays were performed as previously reported (9, 15, 16). Transfection was performed 18 h following seeding for 3 h using Lipofectamine Plus (Invitrogen) and following the manufacturer's protocol. For luciferase studies, cells in 12-well plates were transiently cotransfected with the appropriate plasmids, 100 ng β-galactosidase (internal control vector for normalizing), 900 ng pLucTKS3, pLucSRE, pLucKLF8, or pLucKLF8/−253T/G, and with or without 300 ng pMv-Src. Where appropriate, cells in 96-well plates were transfected with Stat3C (0.2 μg) or in 6-well plates were transfected with 4 μg Stat3C, Stat3 SH2 domain, or pcDNA3 (mock). Twelve hours after transfection, cells were treated or untreated with BP-1-102 (0–30 μM) for 16–48 h and harvested. Subsequently, cytosolic extracts were prepared for luciferase assay or nuclear extracts were prepared for EMSA analysis, as previously reported (9, 15), whole-cell lysates were prepared for immunoblotting analysis, or the cells were processed for CyQUANT cell proliferation or Annexin V/flow cytometry analysis.

The Stat3 siRNA smart pool Stat3 (M-003544) and the control, SiGENOME nontargeting siRNA pool (Dharmacon RNAi Technologies, Thermo Scientific), were transiently transfected into cells using Lipofectamine RNAiMAX (Invitrogen) in serum-free Opti-MEM culture medium (5 mL) (Invitrogen) according to the manufacturer's instructions and using 200 pmol siRNA with 10 μL of Lipofectamine.

Immunoprecipitation and Western Blotting Analyses. Whole-cell lysates or tumor tissue lysates from pulverized tumor tissue were prepared in boiling SDS sample loading buffer to extract total proteins, as reported previously (9, 17, 18). Lysates of equal total protein were electrophoresed on an SDS/7.5% (g/vol) polyacrylamide gel and transferred to a nitrocellulose membrane. Nitrocellulose membranes were probed with primary antibodies, and the detection of horseradish peroxidase-conjugated secondary antibodies by enhanced chemiluminescence (Amersham) was performed. Immunoprecipitation studies were performed as previously reported (7) using whole-cell lysates or nuclear extracts (250 μg total protein) and 2 μg of anti-Stat3, anti–NF-κB/p65RelA, or anti-IκB polyclonal antibody (Santa Cruz Biotechnology) or 5 μL of monoclonal anti-Stat3 antibody (Cell Signaling Technology).

CyQUANT Cell Proliferation, Viability, Colony Survival, and Wound-Healing Assays. These studies were performed as previously reported (1, 16). Briefly, proliferating cells in 6- or 96-well plates were treated once with 0–30 μM BP-1-102 for 24 h or with 10 μM BP-1-102 for up to 96 h. Viable cells were counted by trypan blue exclusion/phase-contrast microscopy or assessed by a CyQUANT Cell Proliferation Kit, according to the manufacturer's (Invitrogen) instructions. For colony-survival studies, cells were seeded as a single-cell culture. On the next day following seeding, cells were treated once or not with BP-1-102 and allowed to culture until large colonies were visible, which were fixed with methanol and stained with crystal violet (Thermo Fisher Scientific) for 2 h. The number of colonies was counted or photomicrographs were taken under a phase-contrast microscope. For wound-healing assays, subconfluent cultures of cells in 6-well plates were wounded using pipette tips and treated with or without BP-1-102 and allowed to migrate into the denuded area over a 16-h period. The migration of cells was visualized at a 10× magnification using an Axiovert 200 inverted fluorescence microscope (Zeiss), with pictures taken using a mounted Canon Powershot A640 digital camera. Cells that migrated into the denuded area were quantified.

Immunostaining with Laser-Scanning Confocal Imaging. Studies were performed as previously reported (19). Briefly, cells were grown on glass coverslips in multiwell plates, fixed with ice-cold methanol for 15 min, washed three times with 1× PBS, permeabilized with 0.2% Triton X-100 for 10 min, and further washed three or four times with PBS. Specimens were then blocked in 1% BSA for 30 min and incubated with anti-pY705Stat3 (Cell Signaling) or anti–pS536NF-κB/p65 (Cell Signaling) antibody at 1:50 dilution (in 0.1% BSA) at 4 °C overnight. Subsequently, cells were rinsed three times with PBS and incubated with two Alexa Fluor secondary antibodies, Alexa Fluor 546 (goat anti-mouse) and Alexa Fluor 488 (donkey anti-rabbit) (Molecular Probes, Invitrogen) for pY705Stat3 and pS536NF-κB/p65 detection, respectively, for 1 h at room temperature in the dark. Specimens were then washed three times with PBS, mounted on slides with VECTASHIELD mounting medium containing DAPI (Vector Labs), and examined immediately under a Leica TCS SP5 confocal microscope. Images were captured and processed using Leica TCS SP 5 software.

KLF8 Knockdown and Overexpression and Cell Migration/Invasion Assays. Cell migration/invasion experiments were carried out and quantified as previously reported (7, 8, 20) using BioCoat migration/invasion chambers (BD Biosciences) of 24-well companion plates with cell-culture inserts containing 8-μm pore size filters and following the manufacturer's protocol, with some modifications. Briefly, for doxycycline (Dox) induction, cells were maintained uninduced (U; in the absence of Dox) or induced (I; in the presence of Dox) for 3 d. Cells were then resuspended in serum-free medium with or without Dox, transferred to the top chambers of the 24-well transwell plates, and incubated for 16 h to allow the migration or invasion toward the serum-containing medium in the bottom chamber, and cells on the lower side were then counted. BP-1-102 (0–10 μM) was added to both the top and bottom chambers during the 16-h incubation. Where appropriate, the migration or invasion rates were normalized to the control, U cells in the absence of serum and in the bottom chambers.

For KLF8 overexpression, lentiviral particles were prepared and packaged following a published procedure (21) by transfecting cultures of HEK293FT cells with tetracycline-inducible KLF8 expression vector, pLVUT-tTR-KRAB-KLF8 (12 μg), and psPAX2 (8 μg) and pMD2G (4 μg) packaging system (Addgene) and following the manufacturer's instructions. For transient in-

fection, the viral particle-containing HEK293FT cell-culture medium was added to MDA-MB-231 cells in culture and incubated for 48 h at 37 °C. Five nanograms per mL tetracycline was added to the culture and further incubated for 24 h. Infected cells were used in a BioCoat invasion chamber assay, as previously published (7, 8, 22), in the presence or absence of different concentrations of BP-1-102.

Cytokine Assay. Cytokine analysis was performed using a Human Cytokine Array Kit and following the manufacturer's (R&D Systems) instructions. Briefly, following treatment of cells with 10 μM BP-1-102 for 48 h, 1-mL samples of conditioned culture medium or, in the case of tumors, 500 μg of tumor tissue lysates in RIPA buffer (50 mM Tris·HCl, pH 7.4, 1% (vol/vol) Nonidet P-40, 150 mM NaCl, 2 mM EDTA, 0.1% SDS), were mixed with a mixture of biotinylated detection antibodies. The mixture was incubated with the array membrane for antibody binding on the membrane. The membrane was processed for signal development using streptavidin-HRP and chemiluminescent detection reagents and exposed to X-ray films, which were then processed. The relative changes in cytokine levels between samples were analyzed by quantitation of pixel density in each spot of the array with ImageJ (National Institutes of Health).

Fluorescence Polarization Assay. This was conducted as previously reported (1, 16). Full-length Stat3 and its peptide probe, the interleukin (IL)-6R/gp130 peptide, have been previously reported (1, 16). Stat1 and Stat5 were purchased from SignalChem. The peptides, GpYDKPHVL-NH_2 and GpYLVLDKW-NH_2, used for Stat1 and Stat5 fluorescence polarization (FP), respectively, were purchased from CanPeptide.

NMR and Isothermal Titration Calorimetry Studies for Effect of BP-1-102 on IL-6R/gp103 pTyr Peptide Binding to Stat3 SH2 Domain. The 1D ^{1}H Carr-Purcell-Meibom-Gill (CPMG) R_2 relaxation filter experiment was conducted at 298K on a Bruker 600-MHz magnet equipped with a cryoprobe (23). Fifty micromolar gp130 phospho-tyrosine peptide (pY904, Ac-pY-LPQTV-NH_2) was dissolved in 20 mM sodium phosphate (pH 3.2), 0.2% DMSO-d_6, and 90% (vol/vol) D_2O. Binding of pY904 to monomeric Stat3 (encompassing residues 127–711) was monitored by the attenuation of the peptide signals in the CPMG experiment with addition of 2 μM Stat3. The CPMG pulse train used a 3-ms interpulse delay and a total R_2 relaxation time of 72 ms, which completely attenuated the Stat3 signal. For the inhibitor interference reaction at the SH2 binding site, 100 μM BP-1-102 was added to the Stat3–pY904 complex. Under these sample conditions, the apparent concentration of soluble and monomeric BP-1-102 was at least 10 μM as judged by a 1D ^{1}H NMR solubility test of 200 μM BP-1-102 at varying concentrations of DMSO-d_6 (0.2–40% vol/vol).

For the isothermal titration calorimetry (ITC) experiments, the same buffer conditions used in the NMR experiment were maintained for 150 μM titrant (pY904 or BP-1-102) and 10 μM STAT3 in the sample cell of a Microcal VP-ITC calorimeter. Titration of Stat3 ligand-precomplexed samples used equimolar amounts of pY904 or BP-1-102 in the sample cell. Titrant solution (290 μL) was injected at 10-μL increments into a sample cell containing 1.4 mL Stat3 at 298K. The heat flow of the titration reactions was measured at each addition of a pY904 or BP-1-102 aliquot to free or ligand-complexed Stat3. Origin software (Microcal) was used to generate the final ITC figures (Fig. S1 *D* and *E*). The area under each titration peak in Fig. S1 *D* and *E* (*Upper*) was integrated (*Lower*) and plotted against the corresponding ligand:Stat3 molar ratio. The *y* intercept of the lower panel plots represents the directly measured enthalpy change (ΔH).

Phospho-Kinase Profiling. Phospho-kinase profiling assay was performed using a Human Phospho-Kinase Array Kit according to the manufacturer's instructions (R&D Systems). Briefly, DMSO or BP-1-102–treated cells were washed twice with ice-cold PBS, and whole-cell lysates were prepared using the lysis buffer provided in the kit. Array membranes were blocked with array buffer 1 and incubated overnight at 4 °C with 400 μg of cell lysate diluted with array buffer 1. The membranes were washed with wash buffer, incubated with the detection antibodies (provided in the kit), and subjected to detection using streptavidin-HRP, according to the instructions. After washing, the membranes were developed with Pierce chemiluminescence reagents (Thermo Fisher Scientific). The developed images were analyzed based on the pixel density of each spot of the array by scanning and quantifying, and expressed as the fold change compared with the control group.

Mice and in Vivo Tumor Studies. Six-week-old female athymic nude mice were purchased from Harlan and maintained in institutional animal facilities approved by the American Association for Accreditation of Laboratory Animal Care. All mice studies were performed under an Institutional Animal Care and Use Committee (IACUC)-approved protocol. Athymic nude mice were injected s.c. in the left flank area with 1×10^6 human breast cancer MDA-MB-231 or non–small-cell lung cancer A549 cells in 100 μL PBS. After 5–10 d, tumors of a 30–100 mm^3 volume were established. Animals with established tumors were grouped so that the mean tumor sizes in all groups were nearly identical and then given BP-1-102 (in 0.05% DMSO in water) at 1 or 3 mg/kg (i.v.) every 2 or every 3 d or 3 mg/kg (oral gavage, 100 μL) every day for 15 or 20 d. Animals were monitored every day, and tumor sizes were measured with calipers and body weights were taken every 2 or 3 d. Tumor volumes were calculated according to the formula $V = 0.52 \times a^2 \times b$, where a is the smallest superficial diameter and b is the largest superficial diameter. For each treatment group, the tumor volumes for each set of measurements were statistically analyzed in comparison with the control (nontreated) group using a paired t test.

Plasma and Tumor Tissue Analysis. BP-1-102 concentrations in mouse plasma and tumor tissue lysates were assayed using a validated analytical procedure via HPLCy (Prominence UHPLC; Shimadzu Scientific Instruments) and LC/MS/MS (API 4000 linear ion trap mass spectrometer; MDS Sciex). The mass spectrometer was operated in a product ion-scanning mode. BP-1-102 solution diluted in methanol was infused directly into the MS source at a flow rate of 10 μL/min. Tuning was evaluated in both positive and negative MS modes using both turbo ion spray and atmospheric pressure chemical ionization sources. The chromatography used a Phenomenex Kinetex C18 2.1 × 50 mm, 1.7 μ UHPLC column, with a flow rate of 0.300 mL/min using 5 mM ammonium acetate (in water) and 5 mM ammonium acetate (in acetonitrile) as mobile phases A and B, respectively.

In Vivo Toxicity Studies. Six-week-old female athymic nude mice were purchased from Harlan and maintained in institutional animal facilities approved by the American Association for Accreditation of Laboratory Animal Care. All mice studies were performed under an IACUC-approved protocol. Groups of three or four healthy mice were administered BP-1-102, i.v. at 1 or 3 mg/kg every 2 or 3 d, as was pursued in the antitumor efficacy studies, for 21 d and monitored for up to 42 d. Body weights were measured every 2 or 3 d. Following completion, mice were euthanized and surgery was performed to expose the abdominal organs, which were subsequently removed for visual examination and imaging by a digital camera.

1. Zhang X, et al. (2010) A novel small-molecule disrupts Stat3 SH2 domain-phosphotyrosine interactions and Stat3-dependent tumor processes. *Biochem Pharmacol* 79:1398–1409.
2. Fletcher S, et al. (2011) Antagonism of the Stat3-Stat3 protein dimer with salicylic acid based small molecules. *ChemMedChem* 6:1459–1470.
3. Razgulin AV, Mecozzi S (2006) Binding properties of aromatic carbon-bound fluorine. *J Med Chem* 49:7902–7906.
4. Ma J, Zhang T, Novotny-Diermayr V, Tan AL, Cao X (2003) A novel sequence in the coiled-coil domain of Stat3 essential for its nuclear translocation. *J Biol Chem* 278:29252–29260.
5. Zhang T, Seow KT, Ong CT, Cao X (2002) Interdomain interaction of Stat3 regulates its Src homology 2 domain-mediated receptor binding activity. *J Biol Chem* 277:17556–17563.
6. Wang X, Urvalek AM, Liu J, Zhao J (2008) Activation of KLF8 transcription by focal adhesion kinase in human ovarian epithelial and cancer cells. *J Biol Chem* 283:13934–13942.
7. Siddiquee KAZ, et al. (2007) An oxazole-based small-molecule Stat3 inhibitor modulates Stat3 stability and processing and induces antitumor cell effects. *ACS Chem Biol* 2:787–798.
8. Siddiquee K, et al. (2007) Selective chemical probe inhibitor of Stat3, identified through structure-based virtual screening, induces antitumor activity. *Proc Natl Acad Sci USA* 104:7391–7396.
9. Turkson J, et al. (1998) Stat3 activation by Src induces specific gene regulation and is required for cell transformation. *Mol Cell Biol* 18:2545–2552.
10. Wagner BJ, Hayes TE, Hoban CJ, Cochran BH (1990) The SIF binding element confers sis/PDGF inducibility onto the c-fos promoter. *EMBO J* 9:4477–4484.
11. Gouilleux F, et al. (1995) Prolactin and interleukin-2 receptors in T lymphocytes signal through a MGF-STAT5-like transcription factor. *Endocrinology* 136:5700–5708.
12. Seidel HM, et al. (1995) Spacing of palindromic half sites as a determinant of selective STAT (signal transducers and activators of transcription) DNA binding and transcriptional activity. *Proc Natl Acad Sci USA* 92:3041–3045.
13. Turkson J, et al. (2001) Phosphotyrosyl peptides block Stat3-mediated DNA binding activity, gene regulation, and cell transformation. *J Biol Chem* 276:45443–45455.
14. Turkson J, et al. (2005) A novel platinum compound inhibits constitutive Stat3 signaling and induces cell cycle arrest and apoptosis of malignant cells. *J Biol Chem* 280:32979–32988.
15. Turkson J, et al. (1999) Requirement for Ras/Rac1-mediated p38 and c-Jun N-terminal kinase signaling in Stat3 transcriptional activity induced by the Src oncoprotein. *Mol Cell Biol* 19:7519–7528.
16. Zhao W, Jaganathan S, Turkson J (2010) A cell-permeable Stat3 SH2 domain mimetic inhibits Stat3 activation and induces antitumor cell effects in vitro. *J Biol Chem* 285: 35855–35865.
17. Turkson J, et al. (2004) Inhibition of constitutive signal transducer and activator of transcription 3 activation by novel platinum complexes with potent antitumor activity. *Mol Cancer Ther* 3:1533–1542.
18. Turkson J, et al. (2004) Novel peptidomimetic inhibitors of signal transducer and activator of transcription 3 dimerization and biological activity. *Mol Cancer Ther* 3: 261–269.
19. Jaganathan S, et al. (2011) A functional nuclear epidermal growth factor receptor, SRC and Stat3 heteromeric complex in pancreatic cancer cells. *PLoS One* 6:e19605.
20. Wang X, et al. (2007) Krüppel-like factor 8 induces epithelial to mesenchymal transition and epithelial cell invasion. *Cancer Res* 67:7184–7193.
21. Sun N, Lee A, Wu JC (2009) Long term non-invasive imaging of embryonic stem cells using reporter genes. *Nat Protoc* 4:1192–1201.
22. Wang X, et al. (2011) KLF8 promotes human breast cancer cell invasion and metastasis by transcriptional activation of MMP9. *Oncogene* 30:1901–1911.
23. Dalvit C, et al. (2002) High-throughput NMR-based screening with competition binding experiments. *J Am Chem Soc* 124:7702–7709.

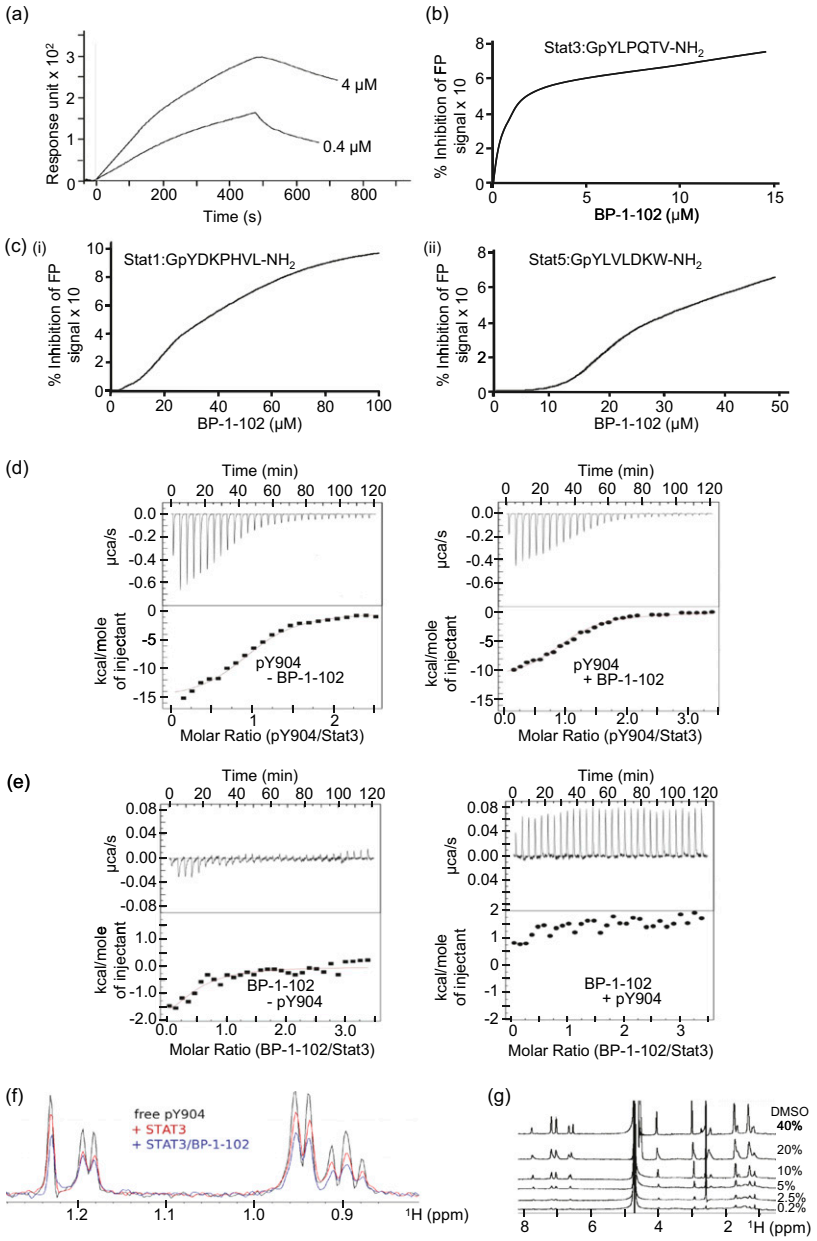

Fig. S1. Characterization of Stat3 binding to BP-1-102 compared with the interaction with the tyrosine-phosphorylated IL-6 receptor/glycoprotein (gp)130 peptide. (*A*) Surface plasmon resonance analysis of the binding of increasing concentrations of BP-1-102 to full-length Stat3. (*B* and *C*) Fluorescence polarization assay of the binding to 10 nM 5-carboxyfluoresceinyl-labeled IL-6R/gp130 peptide (GpYLPQTV-NH_2) (*B*), IFN-γ receptor peptide (GpYDKPHVL-NH_2) (*C*, *i*), or erythropoietin receptor peptide (GpYLVLDKW-NH_2) (*C*, *ii*) probe of a fixed amount of purified His-Stat3 (200 nM), Stat1 (120 nM), or Stat5 (105 nM), respectively, in the presence of increasing concentrations (0–100 μM) of BP-1-102. Inhibition of FP signal is represented as percent inhibition (of control) vs. concentration of BP-1-102. (*D* and *E*) Isothermal titration calorimetry measurements of the binding of (*D*) pY904 to Stat3 in the absence (*Left*) and presence (*Right*) of BP-1-102, or (*E*) BP-1-102 to Stat3 in the absence (*Left*) and presence (*Right*) of pY904. The area under each titration peak (*D* and *E*, *Upper*) is integrated (*Lower*) and plotted against the corresponding pY904:Stat3 or BP-1-102:pY904 molar ratio. The red line is the fit of the binding isotherm to extract the thermodynamic parameters using a one-site binding model. (*F*) Overlay of a section of the 1D ^{1}H R_2 CPMG NMR spectra of 50 μM pY904 alone (black tracing), in the presence of 2 μM Stat3 (red tracing), and together with 100 μM BP-1-102 (blue tracing) at 0.1% DMSO. The CPMG pulse train used a 3-ms interpulse delay and a total R_2 relaxation time of 72 ms, which completely attenuated the Stat3 signal. (*G*) The 1D ^{1}H NMR spectra of 200 μM BP-1-102 at various concentrations of DMSO (0.2–40%) showing broadened signal at reduced DMSO. The apparent concentration of monomeric BP-1-102 is reduced to 10 μM under completely aqueous conditions. Data are representative of two or three independent determinations.

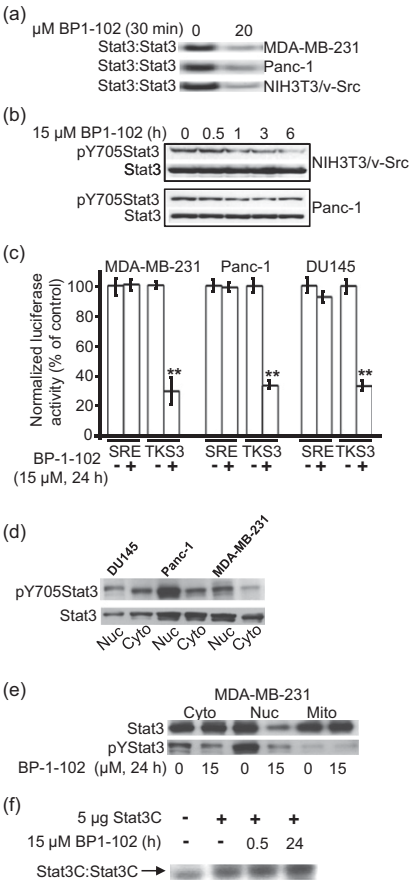

Fig. S2. Effects of BP-1-102 on the induction of Stat3 phosphorylation, intracellular localization, and transcriptional activity. (*A*) EMSA analysis using hSIE probe of Stat3 DNA-binding activity in nuclear extracts of equal total protein prepared from the designated tumor cells treated or untreated with 20 μM BP-1-102 for 30 min. (*B*) Immunoblots of pY705Stat3 and Stat3 in whole-cell lysates of equal total protein prepared from the designated malignant cells treated or untreated with 15 μM BP-1-102 for the indicated times. (*C*) Cytosolic extracts of equal total protein were prepared from 24-h BP-1-102–treated or untreated MDA-MB-231, Panc-1, or DU145 cells transiently transfected with the Stat3-dependent (pLucTKS3, TKS3) or Stat3-independent [pLucSRE, serum response element (SRE)] luciferase reporter and analyzed for luciferase activity using a luminometer. (*D* and *E*) Immunoblotting analysis of lysates of nuclear (Nuc), cytosolic (Cyto), or mitochondrial fractions of equal total protein prepared from the designated tumor cells untreated or treated with 15 μM BP-1-102 for 24 h and probing for pY705Stat3 or Stat3. (*F*) EMSA analysis using hSIE probe of Stat3C DNA-binding activity in nuclear extracts of equal total protein prepared from normal NIH 3T3 fibroblasts transfected with or without Stat3C vector and treated or untreated with 15 μM BP-1-102 for the indicated times. Positions of protein–DNA complex or proteins in the gel are labeled; control (0) or (–) represents extracts or lysates prepared from 0.05% DMSO-treated cells. Data are representative of two to four independent determinations. Values are the mean and SD of three independent determinations each performed in triplicate. For each transfection, luciferase activity was normalized to transfection efficiency, with β-galactosidase activity as an internal control. $^{**}P < 0.01$.

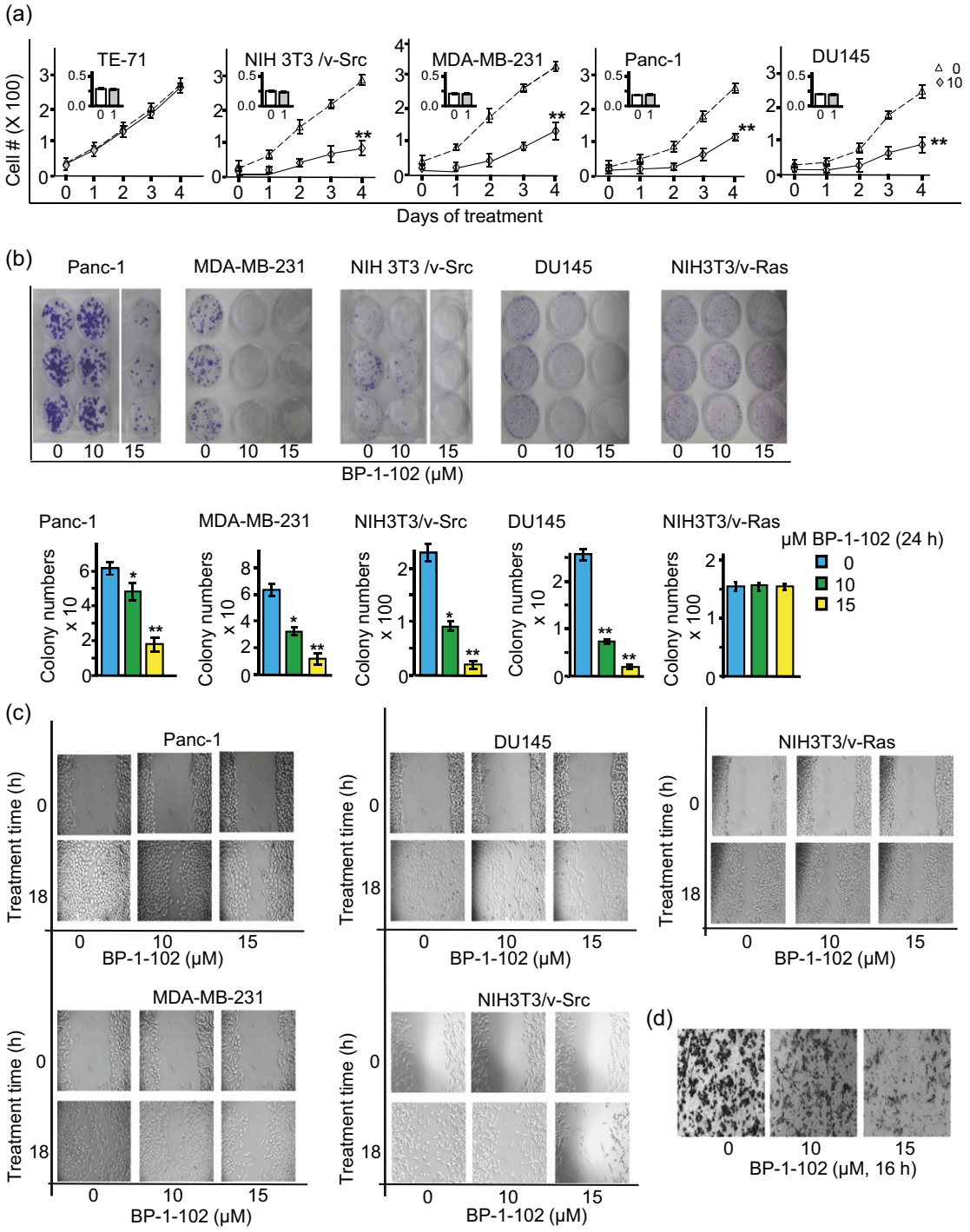

Fig. S3. BP-1-102 selectively suppresses proliferation, survival, migration, and invasion in vitro of Stat3-dependent malignant cells. (*A*–*C*) Tumor cells harboring aberrantly active Stat3 (MDA-MB-231, DU145, Panc-1, and NIH 3T3/v-Src) or cells that do not (NIH 3T3/v-Ras and mouse thymus stromal epithelial cells, TE-71) (*A*) and growing in culture were untreated (dash lines) or treated once with 15 μM BP-1-102 (solid lines) for 24–96 h and the number of viable cells was assessed each day by trypan blue exclusion/phase-contrast microscopy and plotted; (*B*) were seeded as single-cell cultures treated once with 0–15 μM BP-1-102 for 24 h and allowed to culture until large colonies were visible, which were stained with crystal violet and photographed (*Upper*) or enumerated and plotted (*Lower*); or (*C*) were cultured and wounded and treated once with 0–15 μM BP-1-102 for 16 h and allowed to migrate into the denuded area. Cultures were imaged and are represented as photomicrographs. Visualization was done at 10× magnification by light microscopy. (*A*) (*Insets*) Bar graphs of viable cell numbers at day 0 (open bars) and day 1 for BP-1-102–treated cells (filled bars). (*D*) BioCoat migration/invasion chamber assay and the effect of BP-1-102 on the invasiveness of MDA-MB-231 cells. Images were captured under light microscopy with a digital camera. Data are representative of three or four independent determinations. Values are the mean and SD of four independent determinations, each performed in triplicate. $*P < 0.05$, $**P < 0.01$.

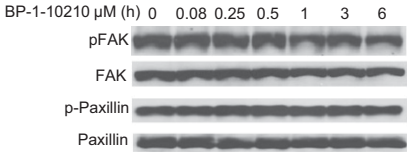

Fig. S4. Time-course study of effects of BP-1-102 on focal adhesion kinase (FAK) and paxillin phosphorylation. Immunoblotting analysis of whole-cell lysates prepared from MDA-MB-231 cells treated with 10 μM BP-1-102 for the indicated times and probing for FAK, phospho-FAK, paxillin, phospho-paxillin, or β-actin. Positions of proteins in the gel are shown. Data are representative of three independent determinations.

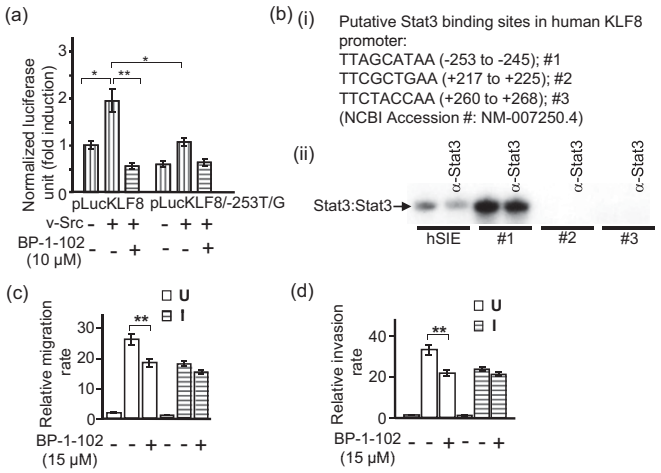

Fig. S5. Transcriptional induction of KLF8 by Stat3 and the effect of BP-1-102. (*A*) Normalized luciferase reporter activity in cytosolic extracts of equal total protein prepared from normal NIH 3T3 fibroblasts transiently transfected with the wild-type KLF8 promoter-driven luciferase reporter, pLucKLF8, or mutant KLF8 promoter-driven reporter, pLucKLF8/-253T/G, together with v-Src and β-galactosidase expression vectors (for internal control), and the effect of 16-h treatment with BP-1-102. (*B*) KLF8 promoter analysis showing (*i*) the nucleotide sequences for the three putative Stat3 binding sites, 1, 2, and 3, and (*ii*) the EMSA analysis of Stat3 DNA-binding activity to the labeled oligonucleotide sequence probes incorporating each of the three putative Stat3 binding sites, compared with the binding to the high-affinity *sis*-inducible element probe using nuclear extract preparations of equal total protein containing activated Stat3 from NIH 3T3/v-Src. (*C* and *D*) BioCoat migration/invasion chamber assay of MDA-MB-231-K8ikd cells harboring inducible KLF8 shRNA and the impact of induced KLF8 knockdown (I) on the BP-1-102 effect on cell (*C*) migration and (*D*) invasion, compared with the wild-type, uninduced (U) cells. Data are representative of three independent determinations. Values are the mean and SD of two or three independent determinations each performed in triplicate. $*P < 0.05$, $**P < 0.01$.

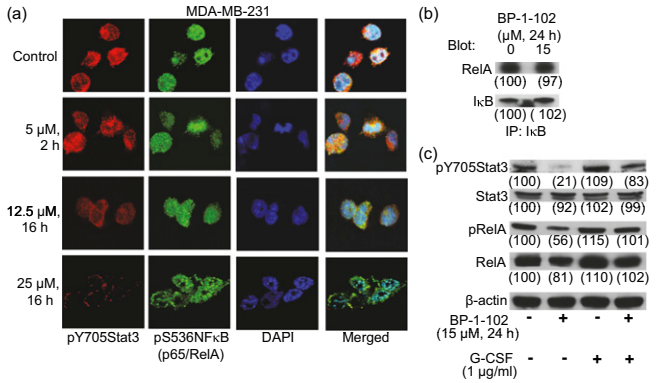

Fig. S6. Effect of BP-1-102 on the activation and localization of NF-κB/p65RelA. (*A*) Immunofluorescence imaging/confocal microscopy of Stat3 colocalization with p65RelA in MDA-MB-231 cells growing in culture and treated with or without 5–25 μM BP-1-102 for 2 or 16 h, fixed, and stained with anti-Stat3 antibody and secondary Alexa Fluor 546 antibody (red), anti-p65RelA and secondary Alexa Fluor 488 antibody (green), or DAPI nuclear staining (blue). Images were captured using a Leica TCS SP5 laser-scanning confocal microscope. (*B*) IκB immunecomplex prepared from MDA-MB-231 cells treated with or without 15 μM BP-1-102 and probing for RelA or IκB. (*C*) Immunoblotting analysis of whole-cell lysates of MDA-MB-231 cells stimulated with G-CSF in the presence or absence of BP-1-102 and probing for pY705Stat3, Stat3, pRelA, RelA, and β-actin. Data are representative of three independent studies. Blots were scanned and quantified by ImageQuant analysis, and numbers represented as percentage of control (100%) are shown in parentheses.

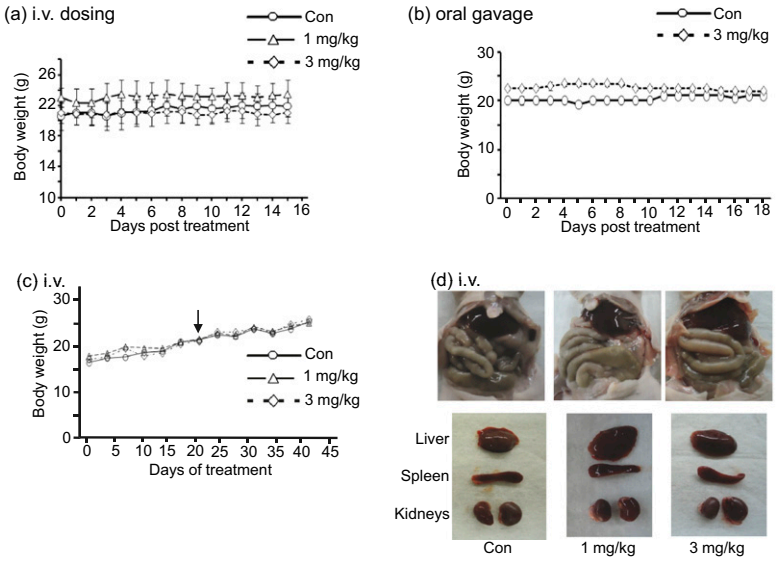

Fig. S7. Evaluation of toxicity of BP-1-102 in mice. (*A* and *B*) Plots of body weight against days of treatment for mice bearing human breast (MDA-MB-231) tumors and treated with BP-1-102 via (*A*) i.v., 1 or 3 mg/kg or vehicle (0.1% DMSO in PBS) every 2 or 3 d or (*B*) oral gavage, 3 mg/kg or vehicle (0.1% DMSO) every day for 14 d. Mice were weighed daily or every 2 d. (*C* and *D*) Healthy mice were treated with BP-1-102 via i.v., 1 or 3 mg/kg or vehicle (0.1% DMSO in PBS) every 2 or 3 d for 21 d and observed for 42 d and (*C*) weights, measured daily or every 2 d, are plotted, or (*D*) images, captured by a digital camera of the internal organs exposed following surgery at the end of the study, are shown. Control (Con or 0) represents 0.05 or 0.1% DMSO-treated mice. Data are representative of four to six mice in each group. Values are the mean and SD of replicates of four to six mice in each group. (*C*) The arrow indicates the last treatment day.

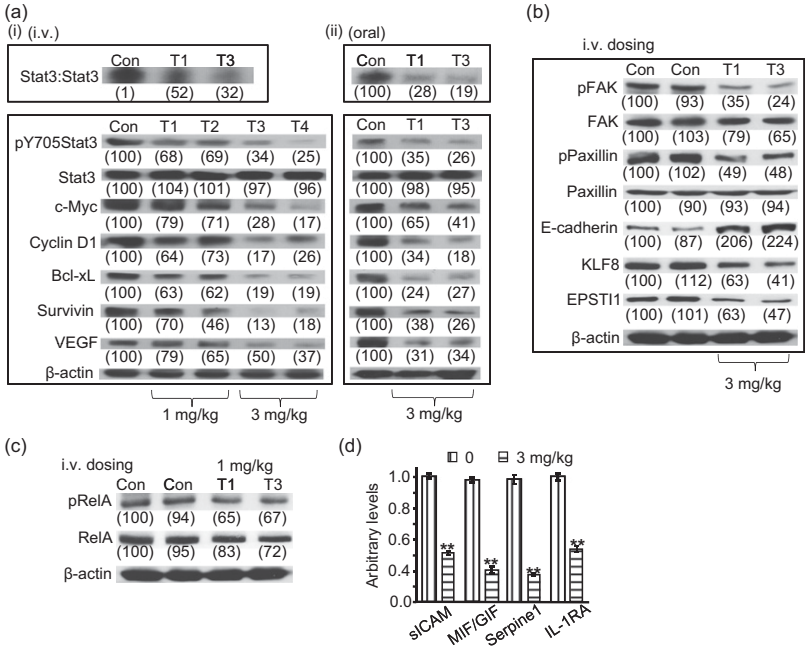

Fig. S8. In vivo treatments with BP-1-102 and effects on Stat3 activity, Stat3-regulated genes, cytokine production, and factors that promote tumor motility, migration, and invasiveness. (*A*–*C*) Tumor lysates prepared from control (Con) human breast tumor xenografts or residual tumor (T1–T4) tissues from mice treated with BP-1-102 (1 or 3 mg/kg) via i.v. or oral gavage were subjected to (*A*, *Upper*) Stat3 DNA-binding activity/EMSA analysis, or (*A*, *Lower*; *B* and *C*) immunoblotting analysis probing for pY705Stat3, Stat3, c-Myc, Cyclin D1, Bcl-xL, Survivin, VEGF, pFAK, FAK, phospho-paxillin, paxillin, E-cadherin, KLF8, epithelial–stromal interaction (EPSTI)1, pRelA, RelA, or β-actin (*D*) Analysis of soluble intercellular adhesion molecule (sICAM), macrophage migration-inhibitory factor (MIG)/glycosylation-inhibiting factor (GIF), Serpine 1, and IL-1RA levels in tumor tissue lysates treated via i.v. Positions of Stat3–DNA complexes or proteins in the gel are labeled; control (Con or 0) represents tumor tissue lysates prepared from 0.05% DMSO-treated mice. Data are representative of three or four independent determinations. Blots were scanned and quantified by ImageQuant analysis, and numbers represented as percentage of control (100%) are shown in parentheses. Values are the mean and SD from replicates of 7–10 tumor-bearing mice in each group. $^{**}P < 0.01$.

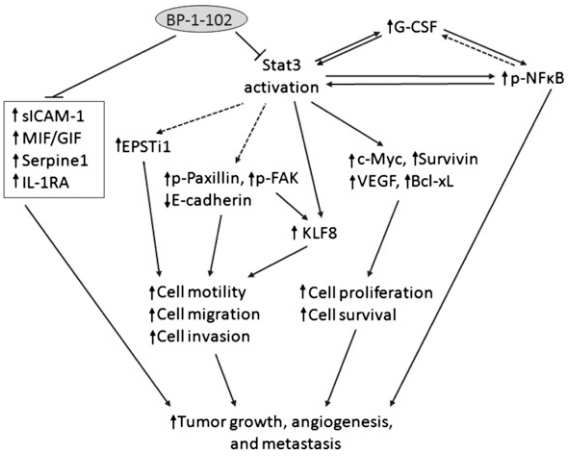

Fig. S9. Model for BP-1-102–mediated molecular changes in malignant cells harboring aberrantly active Stat3 that contribute to antitumor cell effects and the antitumor response. BP-1-102 attenuates aberrant Stat3 signaling and consequently suppresses nuclear Stat3–NF-κB cross-talk and the induction of KLF8, c-Myc, Cyclin D1, Survivin, VEGF, and Bcl-xL. In malignant cells harboring aberrantly active Stat3, BP-1-102 further suppresses FAK and paxillin phosphorylation, EPSTI1 expression, and sICAM, G-CSF, MIF/GIF, Serpine 1, and IL-1RA production, and enhances E-cadherin expression. The modulation of these events would contribute to BP-1-102–induced inhibition of tumor cell growth, survival, motility, migration, invasion, and tumor growth in vivo.

Table S1. Phospho-kinase profile for BP-1-102 effects in MDA-MB-231 cells using a kinase array kit

Kinase	Change relative to untreated control, 1
p38α-T180/Y182	0.8
Erk1/2-T202/Y204, T185/Y187	1.0
JNK pan-Y183/Y185, T221/Y223	1.4
MEK1/2-S218/S222, S222, S226	0.9
MSK1/2-S376/S360	1.1
Akt-S473	1.0
Akt-T308	0.9
GSK-3α/β, S21/S9	0.9
AMPKα1-T174	0.9
AMPKα2-T172	1.1
RSK1/2/3-S380/S386/S377	1.0
RSK1/2-S221/S227	1.0
Pyk2-Y402	1.1
PLCγ-1, Y783	1.0
p70 S6 kinase-T389	1.0
p70 S6 kinase-T421	1.0
p70 S6 kinase-T229	1.0
Src-Y419	1.2
Lyn-Y397	0.8
Lck-Y394	0.9
Yes-Y426	1.1
Fgr-Y412	0.8
Fyn-Y420	1.3